이학석사 학위논문

In situ Nanoparticlization of Conjugated Polymer Synthesized by Cyclopolymerization of 1,6-Heptadiyne Derivatives

1,6-헵타다이아인의 싸이클로폴리머리제이션으로

합성한 전도성 고분자의 자발적인 나노입자화

2013 년 2 월

서울대학교 대학원

화학부 유기화학전공

김 정 은

In situ Nanoparticlization of Conjugated Polymer Synthesized by Cyclopolymerization of 1,6-Heptadiyne Derivatives

지도 교수 최 태 림

이 논문을 이학석사 학위논문으로 제출함
2012 년 12 월

서울대학교 대학원
화학부 유기화학전공
김 정 은

김정은의 이학석사 학위논문을 인준함
2012 년 12 월

위 원 장 _____ 홍 종 인 (인)

부위원장 _____ 최 태 림 (인)

위 원 _____ 손 병 혁 (인)

Abstract

Meldrum's acid has attracted increasing attention from chemists because of its role in a precursor for ketene generation by thermolysis. In this study, we synthesized conjugated polymers containing Meldrum's acid by controlled cyclopolymerization using a third-generation Grubbs catalyst.

To solve the insolubility of the polymer containing Meldrum's acid, copolymerization was used, which eventually provided various soluble random/block copolymers containing Meldrum's acid as well as the conjugated backbone. Interestingly, during block copolymerization, the chain growth of the second block containing Meldrum's acid promoted the *in situ* formation of supramolecules. This was because, as the second block grew longer, not only solvent molecules were excluded but π-π interactions between growing conjugated backbones were stronger. For these strong driving forces, this direct approach provided highly stable core-shell structures without any post-synthetic treatments to induce self-assembly.

Furthermore, in the conjugated polymer core, ketene was generated by thermolysis of Meldrum's acid, followed by consecutively cycloaddition to afford the cross-linked core, which improved the stability of the supramolecules. This was monitored by IR spectroscopy.

Based on this interesting self-assembly phenomenon, we have strived to synthesize block copolymers containing much longer conjugated second block by increasing solubility power of the first block. When the insoluble second block,

polyacetylene segment, was sufficiently long, the structural evolution from spherical core-shell structures to nanocaterpillars could be induced by solvent aging process. This spontaneous nanocaterpillar formation was tracked by changes in UV/vis spectrum, size exclusion chromatography, dynamic light scattering, and atomic force microscopy. To clarify the state of each micelle core, transmission electron microscopy was also used.

Keywords: Cyclopolymerization, Meldrum's acid, In situ Nanoparticlization of Conjugated Polymer, Nano-caterpillar

Student Number: 2011-20289

Contents

Part 1 :

Cyclopolymerization to synthesize Meldrum's acid substituted polyacetylene derivative and in situ nanoparticlization of its block copolymers

1.1 Introduction

Conjugated polymers such as polyacetylene (PA) have been extensively investigated over the past five decades because of the interest in their electric and optical properties,[1] which has opened up the new field of polymer electronics.[2] PA, the simplest conducting polymer, unfortunately suffers from extremely low solubility and processibility, which have limited its applications. In order to increase its solubility and processibility, various substituents have been introduced to the PA backbone. One of the most powerful synthetic strategies for the preparation of soluble and functionalized PA derivatives is the cyclopolymerization of 1,6-heptadiyne derivatives via olefin metathesis.[3] Among many reported catalyst systems, Schrock and Buchmeiser reported the pioneering results of cyclopolymerization of the 1,6-heptadiyne derivatives using well-defined catalysts.[4,5] Recently, our group reported highly efficient living cyclopolymerization of 1,6-heptadiyne derivatives using a user-friendly third-generation Grubbs catalyst, which selectively generated five-membered ring structures.[6] Furthermore, this polymerization allowed for the synthesis of block copolymers with various structures.[7]

Since the first synthesis by Meldrum in 1908,[8] Meldrum's acid derivatives have been exploited in organic chemistry for their unique properties: the high acidity of the methylene proton and their use as precursors to highly electrophilic ketenes which can be produced from flash vacuum pyrolysis of the Meldrum's acid functionality.[9] Recently, Hawker reported the mild preparation of ketenes from polymers containing Meldrum's acid, and these ketenes were used to cross-link the polymer or introduce various functional groups to the polymer chain.[10,11] This strategy was also applied to the synthesis of polyester from a monomer containing Meldrum's acid.[12] Further development of the synthesis of conjugated polymers containing Meldrum's acid should broaden the applications of the chemistry of

Meldrum's acid and the ketenes that can be generated upon its thermolysis. Herein, we report the the synthesis of conjugated polymers containing Meldrum's acid by cyclopolymerization using a third-generation Grubbs catalyst. We demonstrate that living polymerization allowed for random and block copolymerization, and discuss investigations of the self-assembly behavior of the diblock copolymers and their thermolysis to generate ketenes (Scheme 1-1).

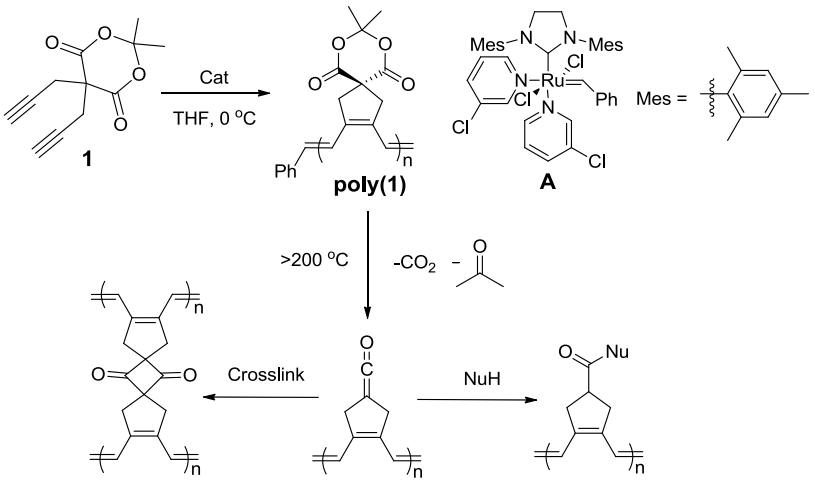

Scheme 1-1. Synthesis of the conjugated polymer containing Meldrum's acid and its post-modification by thermolysis.

1.2 Experimental

1.2.1 General experimental

All reactions were carried out under dry argon atmospheres using standard Schlenk-line techniques. All reagents which are commercially available were used without further purification. 5-norbornene-*endo*-2,3-dicarboxylic anhydride was purchased from Tokyo Chemical Industry, followed by thermal isomerization to the *exo*-form. Solvents for monomer synthesis were also commercially obtained: tetrahydrofuran (THF) was anhydrous (≥ 99.9%) grade from Sigma-Aldrich® . For polymerization, THF was distilled from sodium and benzophenone. THF was degassed for 10 minutes before using on polymerization. Thin-layer chromatography (TLC) was carried out on MERCK TLC silica gel 60 F254 and flash column chromatography was performed using MERCK silica gel 60 (0.040~0.063 mm). ^{1}H NMR and ^{13}C NMR were recorded by Varian/Oxford As-500 (500 MHz for 1H and 125 MHz for 13C) spectrometers. UV–vis spectra were measured by Jasco Inc. UV/vis-Spectrometer V-550. Gel permeation chromatography (GPC) for polymer molecular weight analysis was carried out with Waters system (1515 pump, 2414 refractive index detector and 2489 UV detector) and Shodex GPC LF-804 column eluted with THF (GPC grade, Honeywell Burdick & Jackson). Flow rate was 1.0 mL/min and temperature of column was maintained at 35 ℃. Samples in 0.5-1.0 mg/mL THF were filtered by 0.2-μm PTFE filter before injection. Gel permeation chromatography (GPC) for polymer molecular weight analysis was carried out with Waters system (515 HPLC pump and 2410 refractive refractive index detector), Acme 9000 UV/Vis detector, and Shodex GPC LF-804 column eluted $CHCl_3$ (HPLC grade, J. T. Baker). Flow rate was 0.8 mL/min and temperature of column was maintained at 35 ℃. Samples in 0.5-1.0 mg/mL $CHCl_3$ were filtered by 0.2-μm PTFE filter before injection. High resolution mass spectroscopy (HRMS) analyses were performed by the National Center for Inter-University Research Facility. Multimode 8 and Nanoscope Ⅴ

controller (Veeco Instrument) were used for AFM imaging. Dynamic Light Scattering (DLS) data were obtained by Malvern Zetasizer Nano ZS.

1.2.2 Synthesis of monomers

2,2-dimethyl-5,5-di(prop-2-ynyl)-1,3-dioxane-4,6-dione (1)

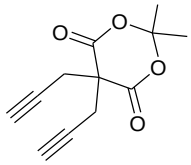

This monomer was prepared by the modified method from the previous literature (S.-H. Jin, H.-N. Cho and S.-K. Choi, *J. Polym. Sci. Polym. Chem. Ed.*, 1993, **31**, 69).Meldrum's acid (2,2-dimethyl-1,3-dioxane-4,6-dione) (720.7 mg, 5 mmol) and K_2CO_3 (99%) (1.728 g, 12.5 mmol) in acetone was prepared in RBF purged with argon. Propargyl bromide (80 wt%, in toluene) (1.23 ml, 11 mmol) was dropwised and stirred for 10 hours with reflux. The mixture was filtered and evaporated, then organic layer was extracted with ethyl acetate (75 mL * 2). The organic layer was dried with $MgSO_4$ and concentrated to give a yellow colored liquid. It was purified by recrystallization with dichloromethane and hexane to afford compound **1** as a white crystalline. (719.7 mg, 3.273 mmol, 65.5 %). ^{1}H-NMR and ^{13}C-NMR data are also available in the same literature. HRMS (CI+): calcd. for $C_{12}H_{13}O_4$, 221.0814, found, 221.0815.

Dihexyl dipropargylmalonate (2)

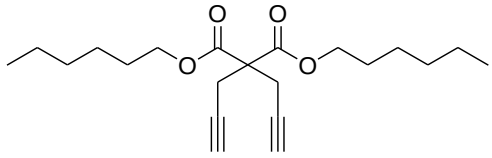

This monomer was prepared by the same method from the previous literature (Kang, E.-H.; Lee, I, S.; Choi, T.-L. *J. Am. Chem. Soc.* 2011, **133**, 11904.). ^{1}H-NMR, ^{13}C-NMR and MS analysis data are also available in the same literature.

***N*-propyl-*exo*-norbornene-5,6-dicarboximide (3)**

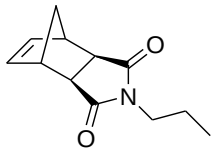

This monomer was prepared by slightly modified method from the previous literature (Meijer, A.; Otto, S.; Engbert, Jan B. F. N. *J. Org. Chem.*, 1998, **63**, 8989.). ^{1}H-NMR, ^{13}C-NMR and MS analysis data are also available in the same literature.

1.2.3 Preparation of catalyst

2nd generation Grubbs catalyst (51.8 mg, 0.0610 mmol) and 3-chloropyridine (1 mL) were mixed in 20-ml sized vial for 5 minutes. Cold *n*-pentane was poured to the vial. After storage in freezer a few hours, the 3rd generation Grubbs catalyst was filtered and washed by pentane. The green product (39.1 mg, 0.0491 mmol, 80.5%) was vacuum dried and stored in desiccator.

1.2.4 General polymerization procedure

Random copolymerization

Monomers (0.1-0.05 mmol) with the given ratios in the table 1 were weighed in a 4-ml sized screw-cap vial with septum and purged with argon. Distilled and degassed solvent (0.2 mL) was added to the vial which was placed in a cold ice bath. The solution of initiator (0.1 mL) was added at once under vigorous stirring. After confirming the monomer conversion by TLC, the reaction was quenched by excess ethyl vinyl ether. The concentrated reaction mixture of poly(**3**)-*ran*-poly(**1**) was precipitated by methanol/isopropylalcohol 1:2 mixture and poly(**2**)-*ran*-poly(**1**) was precipitated by methanol. The obtained solid was dried *in vacuo*

Block copolymerization

Monomer for the 1st block (0.1 mmol) was weighed in a 4-ml sized

screw-cap vial with septum and purged with argon. Anhydrous and degassed solvent (0.1 mL) was added to the vial. The vial was placed in a cold ice bath. The solution of initiator (0.1 mL) was added at once under vigorous stirring. After confirming the monomer conversion by TLC, the solution of **1** (0.2 mL) was added to the vial. After the solution became viscous, the reaction mixture was put in room temperature for 1 hour to assure the full conversion of **1**. The reaction was quenched by excess ethyl vinyl ether and diluted by chloroform to make homogeneous polymer solution. The con-centrated reaction mixture of poly(**3**)-*b*-poly(**1**) was precipitated by methanol/isopropylalcohol 1:2 mixture and poly(**2**)-*b*-poly(**1**) was precipitated by methanol. The obtained solid was dried *in vacuo*

1.2.5 Atomic Force Microscopy (AFM)

The atomic force microscopy experiments were performed with a thin film prepared by spin-coating of one drop of the polymer solution (~0.01 mg/ml, $CHCl_3$, spinning rate = 2000 rpm for 30 sec.). The polymer solution was filtered by 0.2-μm PTFE filter before spin-coating. The thin films were prepared on mica. Images were obtained on tapping mode using non-contact mode tips from Nanoworld (Pointprobe® tip, NCHR type) with spring constant of 42 N m^{-1} and tip radius of ≤8 nm.

1.3 Result and Discussion

1.3.1 Synthesis of random copolymer

To synthesize the conjugated polymer containing Meldrum's acid functionalities, we prepared a 1,6-heptadiyne monomer (**1**) via simple alkylation of Meldrum's acid. Initially, cyclopolymerization of **1** was carried out in THF with a molar feed ratio of **1** to Grubbs catalyst **A** of 50:1. The polymer, poly(**1**), precipitated out as a dark red solid in high yield, but was insoluble in organic solvents such as chloroform and THF.[13] Because of the insolubility of the polymer, no further characterization by ^{1}H NMR and size-exclusion chromatography (SEC) was possible.

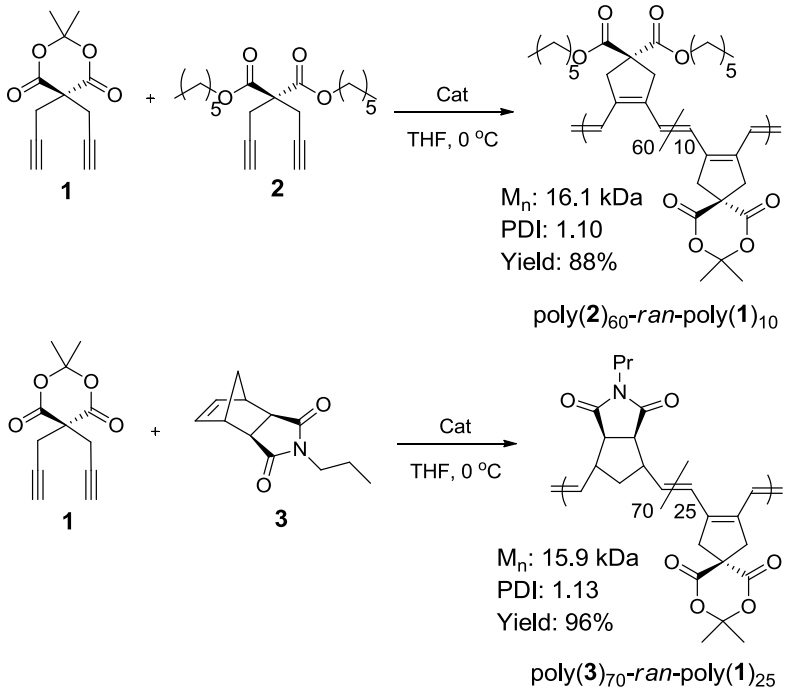

Scheme 1-2. Cyclopolymerization for the synthesis of random copolymers containing Meldrum's acid.

As a strategy to prepare soluble conjugated polymers containing Meldrum's acid, we attempted random copolymerization of **1** with soluble

monomers **2** and **3** using catalyst **A** (Scheme 1-2). First, random copolymerization of **1** and **2** via cyclopolymerization was carried out to yield poly(**2**)-*ran*-poly(**1**). A second random copolymer, poly(**3**)-*ran*-poly(**1**), was synthesized via cyclopolymerization of **1** and ring-opening metathesis polymerization (ROMP) of **3**. In both cases, soluble random copolymers were obtained in high isolated yields at 0 ℃ within 2 hours and ^{1}H NMR analysis showed that the actual incorporated composition matched well with the monomer feed ratios (Figure 1-1).

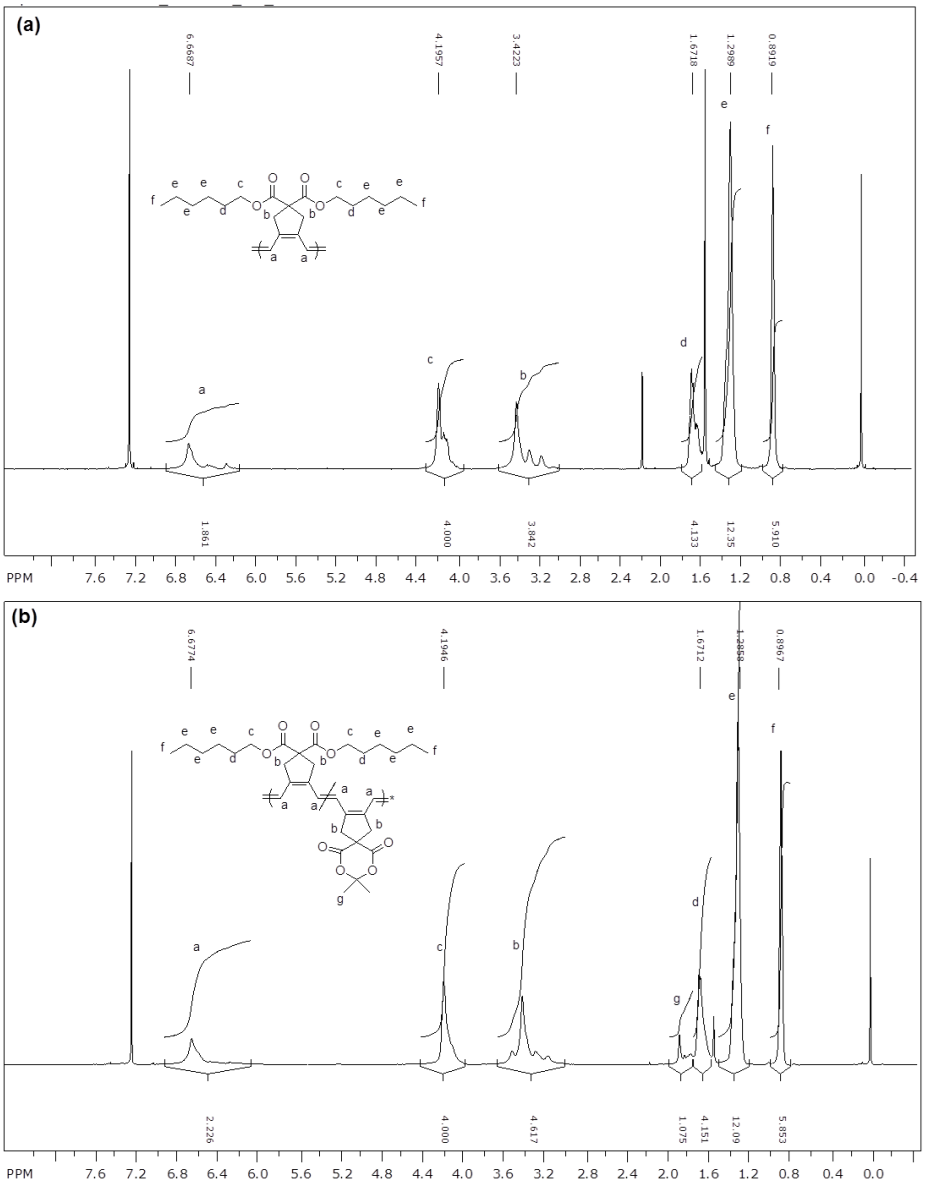

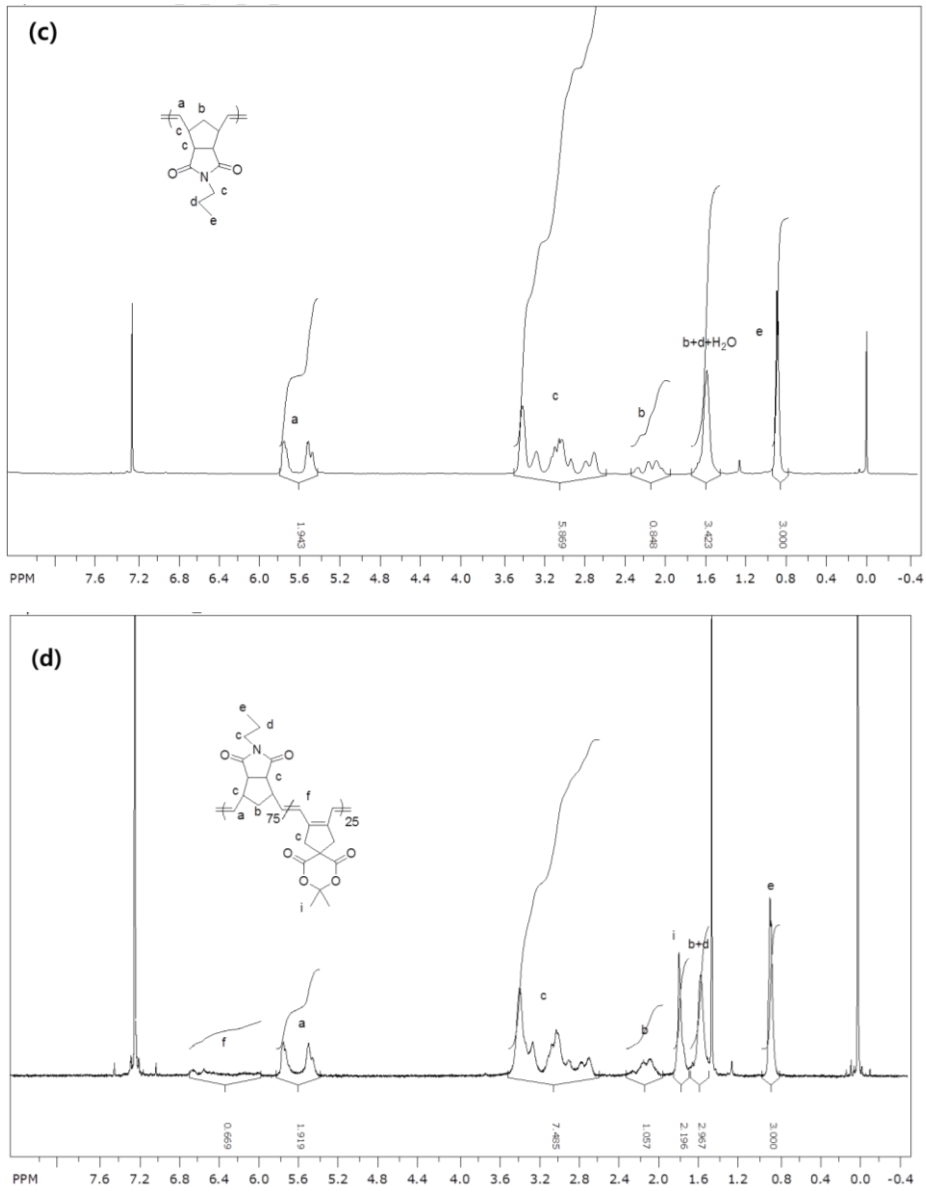

Figure 1-1. ^{1}H NMR peaks for (a) poly(**2**), (b) poly(**2**)$_{60}$-*ran*-poly(**1**)$_{10}$, (c) poly(**3**), and (d) poly(**3**)$_{75}$-*ran*-poly(**1**)$_{25}$. Integration analysis indicated that monomer feed ratio matched well with actual incorporated composition.

Fully conjugated copolymer poly(**2**)-*ran*-poly(**1**) was successfully obtained by random cyclopolymerization and this was confirmed by UV analysis (Figure 1-2a). However, the UV analysis clearly revealed that poly(**3**)-*ran*-poly(**1**) showed a blue shifted absorption spectrum because the

copolymer prepared by ROMP and cyclopolymerization contained a large segment of non-conjugated polymer with only a small polyacetylene segment resulting in short conjugation length (Figure 1-2b). In both cases, narrow polydispersity indice (PDI) below 1.13 determined by the SEC analysis suggested that all three monomers were successfully copolymerized by the living polymerization mechanism.

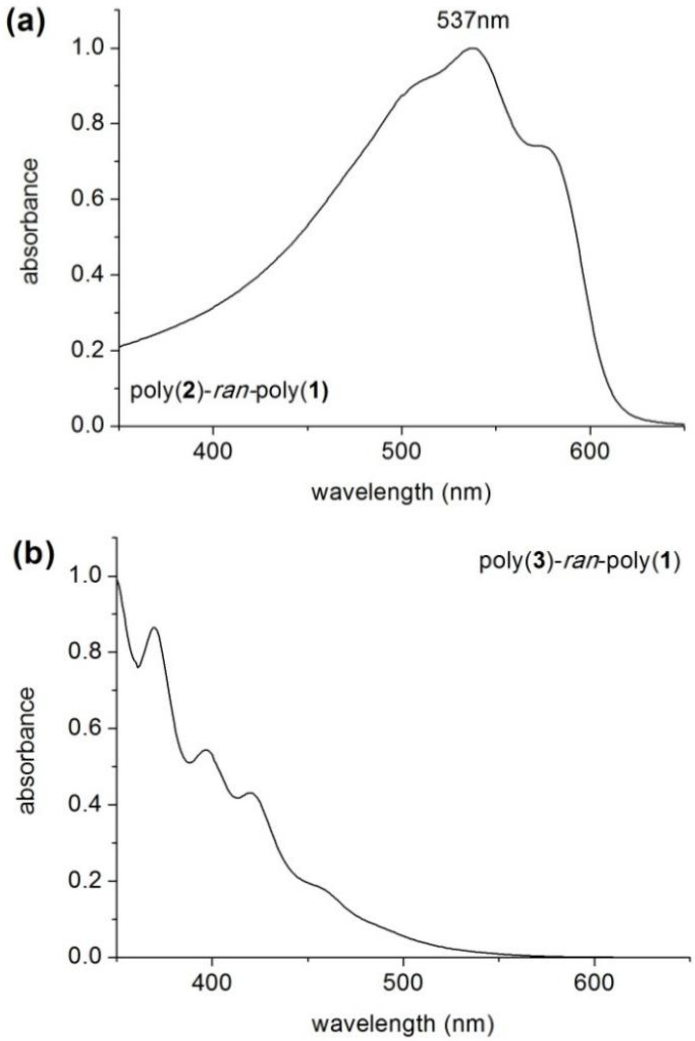

Figure 1-2. UV-vis spectra of (a) poly(**2**)$_{60}$-*ran*-poly(**1**)$_{10}$ and (b) poly(**3**)$_{70}$-*ran*-poly(**1**)$_{25}$ in chloroform solution (0.1 mg/ml).

1.3.2 Synthesis of block copolymer

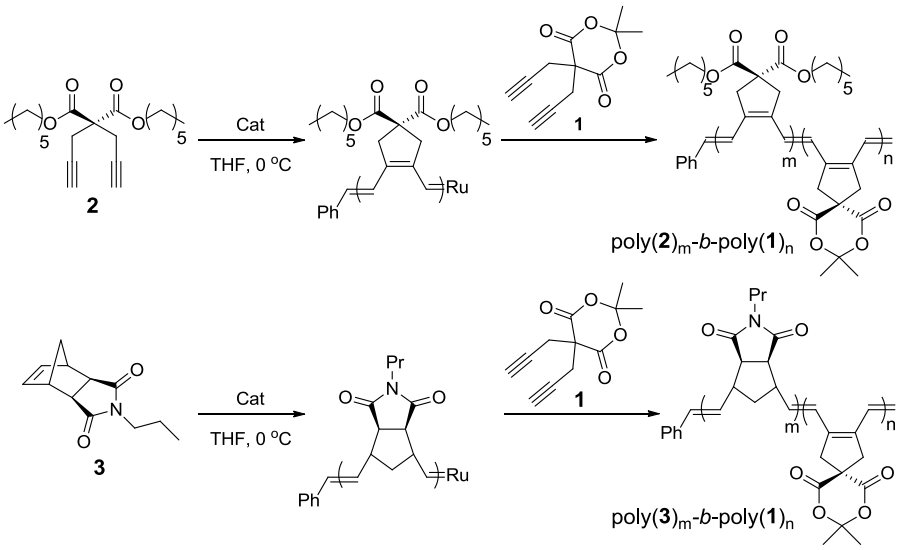

Entry	co-monomer	[co-monomer]:[**1**]:[**A**]	$M_{n,m}$ (kDa)[a]	PDI_m[a]	$M_{n,s}$ (kDa)[b]	PDI_s[b]	Yield (%)[c]
1	**2**	50:25:1	483.4	1.25	18.5	1.12	99%
2	**3**	66:25:1	122.1	1.18	14.5	1.08	98%
3	**3**	100:50:1	352.6	1.57	29.0	1.03	94%

[a] Values corresponding to the micelle. [b] Values corresponding to the polymer single chain determined by SEC eluted by THF and calibrated using polystyrene (PS) standards. [c] Isolated yields after purification.

Table 1-1. Block copolymerization of poly(**1**) with poly(**2**) and poly(**3**).

With the successful random copolymerization of **1** in the living polymerization manner, we attempted the synthesis of diblock copolymers containing poly(**2**) or poly(**3**) as the first block and poly(**1**) as the second block (Table 1). During the synthesis of poly(**2**)-*b*-poly(**1**) (entry 1), there was no clear change in color upon the addition of **1** after the synthesis of the first block of poly(**2**)**.** In contrast, during the synthesis of poly(**3**)-*b*-poly(**1**) (entries 2 and 3), a drastic color change to dark red occurred after the addition of **1**. In

all cases, as **1** was consumed, viscosity of the solution drastically increased suggesting that there was a large increase in the molecular weights of the products. After simple precipitation, the diblock copolymers were obtained in high isolated yields and they were soluble in various organic solvents such as THF, dichloromethane, and chlorobenzene. However, ^{1}H NMR analysis of these block copolymers revealed no signals corresponding to poly(**1**) and only showed signals corresponding to the homopolymers of **2** or **3**, even though the cyclopolymerization of **1** as the second block occurred with full conversion (Figure 1-3).

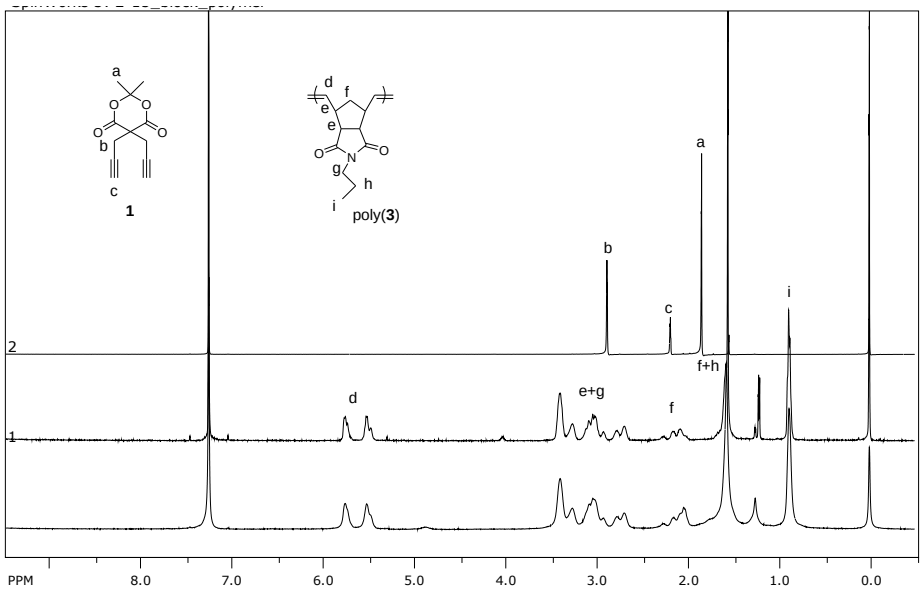

Figure 1-3. ^{1}H NMR peaks for **1**, poly(**3**), and poly(**3**)-*b*-poly(**1**) from the top. spectrum of poly(**3**) overlayed with that of poly(**3**)-*b*-poly(**1**).

These two observations indicated that polymerization-induced self-assembly[14] occurred during block copolymerization to afford supramolecules consisting of the insoluble poly(**1**) block as the core and the soluble poly(**2**) or poly(**3**) block as the shell. SEC analysis of the block copolymers showing two sets of traces strongly supported this idea; major traces with much higher molecular weights ($M_{n,m}$ in Table 1) than expected for the single chain of diblock copolymers ($M_{n,s}$ in Table 1) corresponded to the supramolecules containing the poly(**1**) core (Figure 1-4b). The fact that the majority of the

diblock copolymers maintained their structures as supramolecular adducts even under the high shear force condition of SEC pressure[15] indicated that the supramolecules were highly stable in solution as a result of strong π-π interactions in the conjugated polymer core as well as the insolubility of the second block.

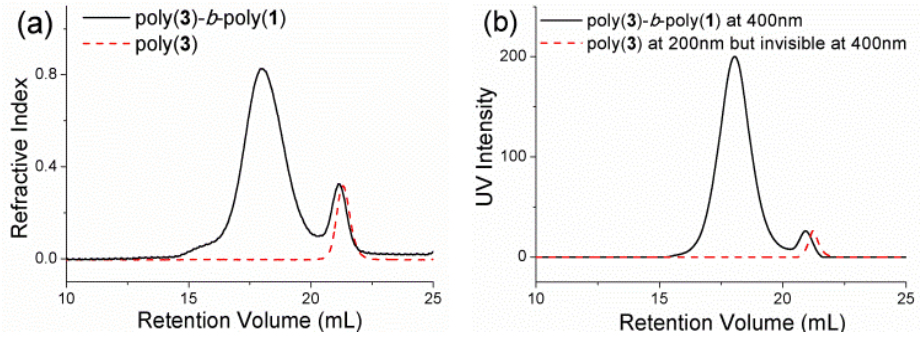

Figure 1-4. (a) $CHCl_3$ SEC traces of poly(**3**) and poly(**3**)-*b*-poly(**1**) determined using an RI detector. (b) SEC traces of poly(**3**)-*b*-poly(**1**) determined using UV detectors. From the SEC analysis with UV detection, we concluded that the minor traces corresponded to the single polymer chain of the diblock copolymers which had slightly shorter PA chain[16] and the major traces with much higher molecular weights corresponded to the supramolecules.

The polymers with high and low molecular weight fraction were separated by SEC and their UV spectra were obtained. (Figure 1-5) The spectrum for the low molecular weight fraction was slightly blue-shifted, but the second block might be long enough to form the core-shell adducts as there was no signals corresponding to the single polymer chain from DLS. (Figure 1-7)

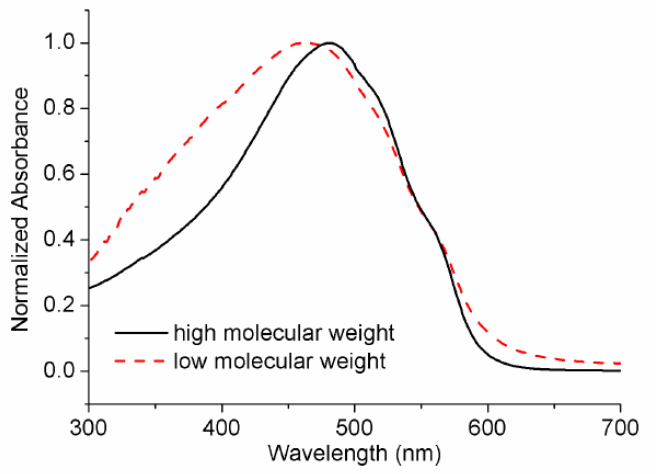

Figure 1-5 UV–vis spectra of poly(**3**)-*b*-poly(**1**) in chloroform solution containing high and low molecular weight fractions after they were separated by SEC. The low molecular weight fraction still contained the conjugated block with slightly lower conjugation length in the second block as it showed a lower λ_{max} peak.

1.3.3 Analysis of core-shell structure by In situ Nanoparticlization of Conjugated Polymer

To investigate the self-assembly in detail, structural information on these supramolecules was obtained using atomic force microscopy (AFM) and dynamic light scattering (DLS) analysis. For AFM imaging, dilute solution of the polymers in chloroform was spin-coated onto mica and via tapping mode, nanospheres with average width of 31.4 (±2) nm and height of 2.4 (±0.7) nm were vividly observed (Figure 1-6a). In addition, the 3-dimensional side-view showed the typical flattened pancake shape of the nanospheres (Figure 1-6b).

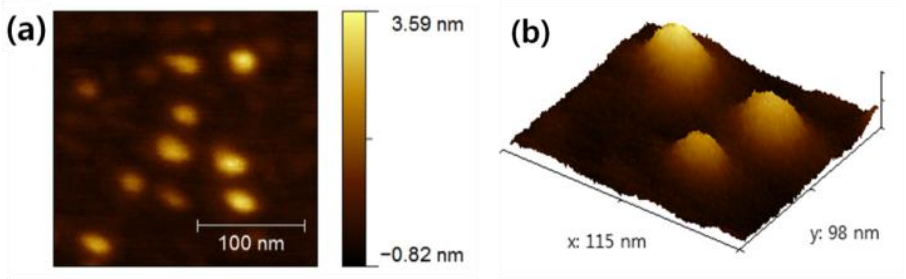

Figure 1-6. (a) AFM image of poly(**3**)$_{100}$-*b*-poly(**1**)$_{50}$ in height mode. The nanospheres had an average width of 31.4 (±2) nm and height of 2.4 (±0.7) nm. (b) Three-dimensional view of the block copolymer micelles.

Next, DLS analysis providing size information revealed that the nanospheres had an average diameter of 45 nm in chloroform solution. The size of the nanospheres determined from the DLS analysis appeared to be larger than that obtained from the AFM images in solid state because of solvation of the polymers in solution (Figure 1-7).

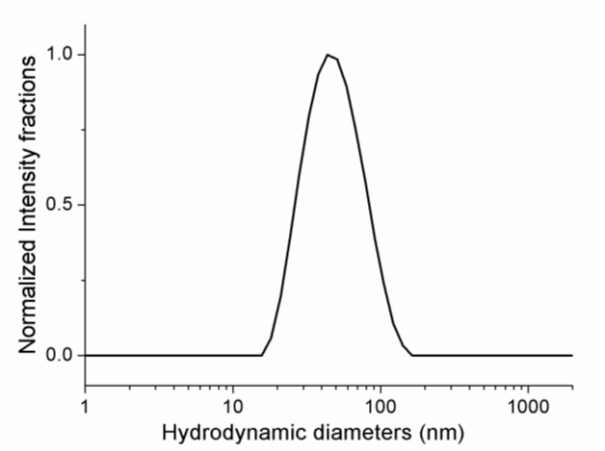

Figure 1-7. Hydrodynamic radius diagram from the solution of poly(**3**)$_{100}$-*b*-poly(**1**)$_{50}$ in $CHCl_3$ (1 mg/ml) obtained by dynamic light scattering. Average hydrodynamic diameter is 44.8 nm.

Surprisingly, the spherical nanostructure was maintained even after heating the solution to 100 ^{o}C or sonicating it for 30 mins. In short, all these analyses strongly indicate that the diblock copolymers spontaneously self-assembled into spherical structures during polymerization. This is because the

growing chain of the insoluble polyacetylene block containing the Meldrum's acid functionalities could no longer be solvated as a unimer and instead formed a spherical supramolecule to reduce the exposed area of the solvophobic PA segment. This process is noteworthy since it eliminates the need for any post-treatments, such as dialysis or changing the specific solvent composition,[16-18] which are essential for inducing the conventional self-assembly process. This direct fabrication of the nanosphere is possible because the π-π interaction forming the core-shell nanostructure is strong enough to maintain the supramolecular adducts even under the shear pressure conditions of SEC.

1.3.4 Ketene generation by thermolysis of Meldrum's acid substituent

With the successful copolymerization of **1**, we next investigated the thermolysis of the various copolymers to monitor the decomposition of Meldrum's acid to ketene. Ketene formation temperatures (T_{kf}) of the random and diblock copolymers containing Meldrum's acid, and the homopolymer of **1** were determined by the onset point in thermal gravimetric analysis (TGA). The clear drop in weight was attributed to the loss of acetone and CO_2 as the ketene was generated, and the observed weight percentages lost were in good agreement with the theoretically calculated weight losses. The T_{kf} of the copolymers (203 ℃ for random and 205 ℃ for block copolymers) were higher than that of the homopolymer (194 ℃) (Figure 1-8a). Direct evidence of ketene formation was confirmed by infrared (IR) analysis of the films of the random and diblock copolymers. After heating the polymer samples at 220 ℃ for 5 minutes, the IR signal at 2111 cm^{-1} corresponding to the ketene appeared,[10] and the signal at 1741 cm^{-1} corresponding to the ester of the Meldrum's acid functionality decreased. For poly(**3**)-*b*-poly(**1**), the signal for the thermally generated ketenes remained for more than 10 hours under ambient conditions (Figure 1-8b). However, for poly(**3**)-*ran*-poly(**1**), the signal for the ketenes disappeared at a much faster rate. We believe that the

increased ketene stability in the block copolymer could be attributed to its core-shell supramolecular structure. The poly(**3**) block would suppress the approach of external nucleophiles such as water to the core. Moreover, well-stacked and solvophobic PA block in the core also prevented nucleophiles from attacking the ketenes. This observation implied that the polymer structures and morphology could be a determining factor for the stability of the ketenes.

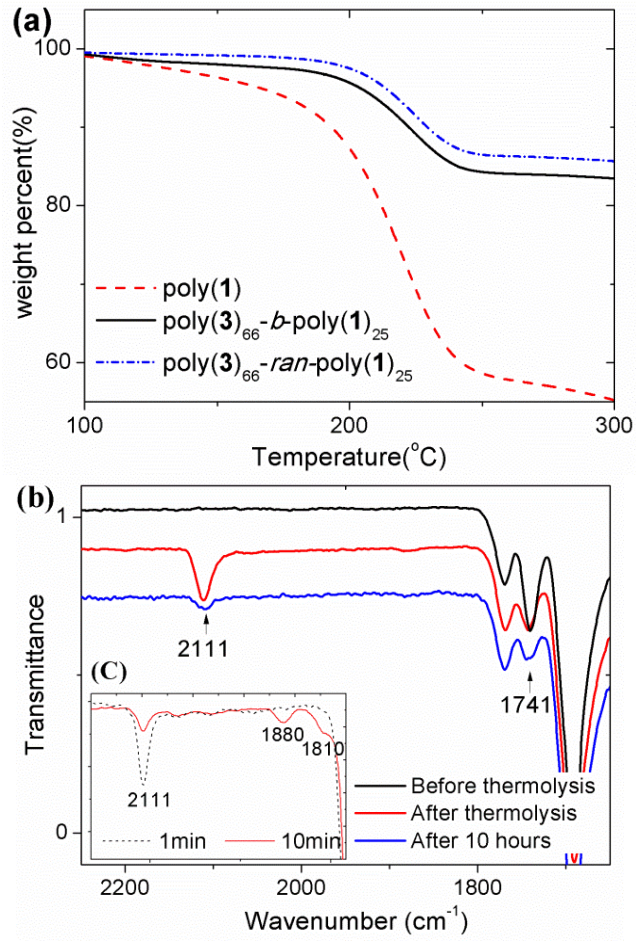

Figure 1-8. (a) TGA profiles of the homopolymer and copolymers. (b) IR spectrum of poly(**3**)-*b*-poly(**1**) to monitor ketene formation before and after thermolysis at 220 ℃ for 5 minutes. The growing signal at 2111 cm^{-1} corresponds to ketene formation and the decreasing signal at 1741 cm^{-1} indicates decomposition of Meldrum's acid. (c) Infrared spectrum of poly(**3**)-*b*-poly(**1**) after heating at 240 ℃ for 1 and 10 minutes. New signals at 1810

cm^{-1} and 1880 cm^{-1} suggest the cross-linking of ketenes to afford cyclobutanedione moieties.

Ketenes are known to undergo [2+2] cycloaddition to give cyclobutanedione[10] (Scheme 1-1). This reaction could be used to permanently cross-link the cores of the nanopspheres. This was achieved by thermolysis of poly(**3**)-*b*-poly(**1**) at 240 ℃ for 10 minutes. This was also monitored by IR analysis, which revealed the reduction in the ketene signal at 2111 cm^{-1} in addition to the apperance of new signals at 1880 cm^{-1} and 1810 cm^{-1} corresponding to cyclobutanedione (Figure 1-8c). To our knowledge, this is the first example of core-shell supramolecules containing a conjugated backbone cross-linked by ketenes generated *in situ*. Although the stable nanospheres were formed directly during the polymerization without post-treatment, this simple cross-linking of the core via heating provides an alternative strategy to photo-cross-linking or covalent cross-linking by click reaction[19-21] to assure an even higher stability of the nanoparticles.

1.4 Conclusion

In conclusion, we have prepared both soluble random and diblock copolymers containing conjugated polymer backbones with the Meldrum's acid functionality via controlled cyclopolymerization using a third-generation Grubbs catalyst. Diblock copolymers containing poly(**1**) as the second block spontaneously self-assembled in organic solvents to generate nanospheres via in situ nanoparticlization of conjugated polymer. Transformation of Meldrum's acid to ketenes occurred successfully by thermolysis at 220 ℃ resulting in highly stable spherical nanoparticles with cross-linked cores. These conjugated polymers containing ketenes could be potentially useful as electronic materials because they consist of semiconducting (and potentially conducting) cores with insulating shells.

Part 2 :

Spontaneous nanocaterpillar formation of spherical micelles prepared by *in situ* nanoparticlization of conjugated polymer

2.1 Introduction

Meldrum's acid is well-known as a precursor generating ketene by thermolysis, and the ketene is labile for the introduction of various functional groups by the reaction with external nucleophile. Previously, we reported the synthesis of conjugated polymers containing Meldrum's acid by cyclopolymerization using a third-generation Grubbs catalyst. To solve the solubility problem of Meldrum's acid substituted PA derivatives, we succeeded in the synthesis of random or block copolymers using copolymerization with ROMP or cyclopolymerization comonomers (Scheme 2-1). We observed the in situ nanoparticlization of block copolymer which contains soluble poly-norbornene block and insoluble, solvophobic PA derivative with Meldrum's acid subsitituent affording to spherical core-shell structure (Figure 2-2).

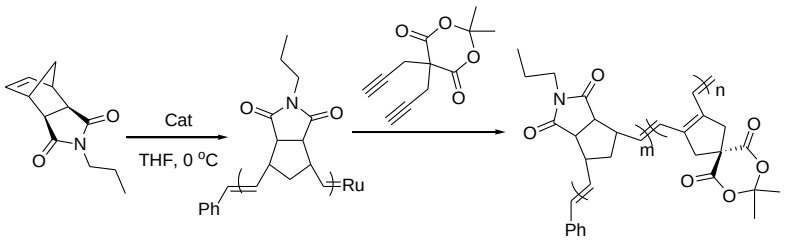

Scheme 2-1. Synthesis of block copolymer containing conjugated polymer with Meldrum's acid substituent

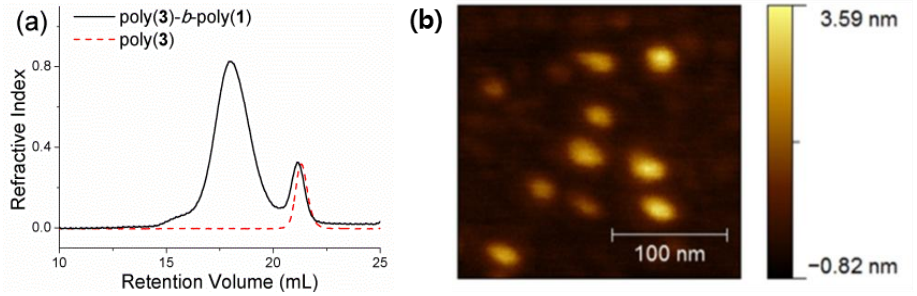

Figure 2-1. (a) $CHCl_3$ SEC traces of block copolymer maintaining its core-shell structure under SEC shear pressure (b) AFM images of spherical micelle

Interestingly, block copolymer containing Meldrum's acid substituted PA derivative as a core showed UV–vis spectrum which is relatively blue-shifted spectrum and shorter λ_{max} than other conjugated polymer synthesized by cyclopolymerization.[6, 22] To investigate this characteristic optical properties, we tried to synthesize block copolymers with various length of PA derivatives. To increase the DP of solvophobic PA derivative block, the substituents of norbornene-based ROMP monomer was changed by much soluble silyl ether group. When the DP of PA derivatives increased up to 100, we observed spontaneous nanocaterpillar formation of spherical core-shell structure by solvent aging under ambient condition.

Herein, we analyzed how the spherical core-shell structure which was formed by in situ nanoparticlization of block copolymer containing conjugated polymer grew to nanocaterpillar in solution state. We characterized the nanostructure formed by solvent aging using DLS, SEC, AFM, and TEM. In addition, we studied the relationship between nanostructure of micelles and the conformational change of conjugated polymer synthesized by cyclopolymerization, and corresponding change in UV–vis spectrum.

2.2 Experimental

2.2.1 General experimental

All reactions were carried out under dry argon atmospheres using standard Schlenk-line techniques. All reagents which are commercially available were used without further purification. 5-norbornene-*endo*-2,3-dicarboxylic anhydride was purchased from Tokyo Chemical Industry, followed by thermal isomerization to the *exo*-form. Solvents for monomer synthesis were also commercially obtained: tetrahydrofuran (THF) was anhydrous (≥ 99.9%) grade from Sigma-Aldrich® . For polymerization, THF was distilled from sodium and benzophenone. THF was degassed for 10 minutes before using on polymerization. Thin-layer chromatography (TLC) was carried out on MERCK TLC silica gel 60 F254 and flash column chromatography was performed using MERCK silica gel 60 (0.040~0.063 mm). ^{1}H NMR and ^{13}C NMR were recorded by Varian/Oxford As-500 (500 MHz for 1H and 125 MHz for 13C) spectrometers. UV–vis spectra were measured by Jasco Inc. UV/vis-Spectrometer V-550. Gel permeation chromatography (GPC) for polymer molecular weight analysis was carried out with Waters system (1515 pump, 2414 refractive index detector and 2489 UV detector) and Shodex GPC LF-804 column eluted with THF (GPC grade, Honeywell Burdick & Jackson). Flow rate was 1.0 mL/min and temperature of column was maintained at 35 ℃. Samples in 0.5-1.0 mg/mL THF were filtered by 0.2-μm PTFE filter before injection. Multimode 8 and Nanoscope Ⅴ controller (Veeco Instrument) were used for AFM imaging. Hitachi 7600 was used for transmission electron microscopy analysis. Dynamic Light Scattering (DLS) data were obtained by Malvern Zetasizer Nano ZS.

2.2.2 Synthesis of monomers

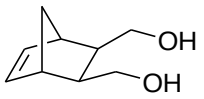

5

5-norbornene-*endo*-2,3-dicarboxylic anhydride was purchased from Tokyo Chemical Industry, followed by thermal isomerization to the *exo*-form. 5-norbornene-*endo*-2,3-dicarboxylic anhydride (1.64 g, 10 mmol) was prepared in RBF purged with argon, and dissolved in THF. Lithium aluminum hydride (474 mg, 12.5 mmol) was added at 0oC and stirred for 16 hours under argon atmosphere. The reaction was quenched by adding ethyl acetate and water (1 mL) then filtered and organic layer was extracted with ethyl acetate (75 mL * 3). The organic layer was dried with $MgSO_4$ and concentrated. It was purified column chromatography with ethyl atetate and hexane (1:1) to afford compound **5** as a colorless liquid (761.5 mg, 5.07 mmol, 50.7 %).

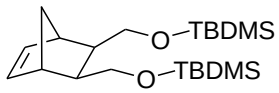

4

5 (761.5 mg, 5.07 mmol) was prepared in RBF purged with argon, and dissolved in DMF (13 mL). Triethyl amine (4.24 mL, 30.4 mmol) was added, and t-butyldimethylsilyl chloride (1.987 g, 13.2 mmol) was added at 0^oC. Finally, dimethylaminopyridine (30.9 mg, 0.25 mmol) was added and stirred overnight at room temperature. The reaction was quenched with ammonium chloride aqueous solution, and organic layer was extracted with ether (50 mL * 2) and water (50ml * 2). The organic layer was dried with $MgSO_4$ and concentrated. It was purified column chromatography with hexane to afford compound **4** as a colorless liquid (1.561 g, 4.12 mmol, 81.3 %)

2.2.3 Atomic Force Microscopy (AFM)

The atomic force microscopy experiments were performed with a thin film prepared by spin-coating of one drop of the polymer solution (~0.01 mg/ml, chlorobenzene, spinning rate = 3000 rpm for 60 sec.). The polymer solution was not filtered before spin-coating. The thin films were prepared on mica. Images were obtained on scan-assyst mode using non-contact mode tips from Nanoworld (Pointprobe® tip, NCHR type) with spring constant of 42 N

m^{-1} and tip radius of ≤8 nm.

2.2.4 Transmittance Electron Microscopy (TEM)

The samples for TEM were prepared by drop-casting 10 μL aliquot of the polymer solution (0.003 mg polymer/mL chlorobenzene) onto a carbon coated copper grid which was placed on a piece of paper to get rid of excess solvent. This polymer thin film was dried in vacuo for 20 h. The images were obtained on Hitachi 7600.

2.3 Result and Discussion

Our first goal was to synthesize block copolymer consisting of longer solvophobic, Meldrum's acid substituted PA derivative (poly(**1**)) block to see the effect on the nanoparticlization phenomena. Unfortunately, the monomer in previous report, which was norbornene with N-propyl succinimide substituent, had a limitation in the synthesis of block copolymer containing long poly(**1**) block with the ratio beyond 100 to 100 because of the reduced solubility. Introduction of *t*-butyldimethylsilylether group as a substituent on norbornene enabled to increase the DP of poly(**1**) block up to 150, but the solubility of block copolymers with higher DPs of poly(**1**) block was too low to dissolve them in organic solvent such as chloroform and chlorobenzene without sonication.

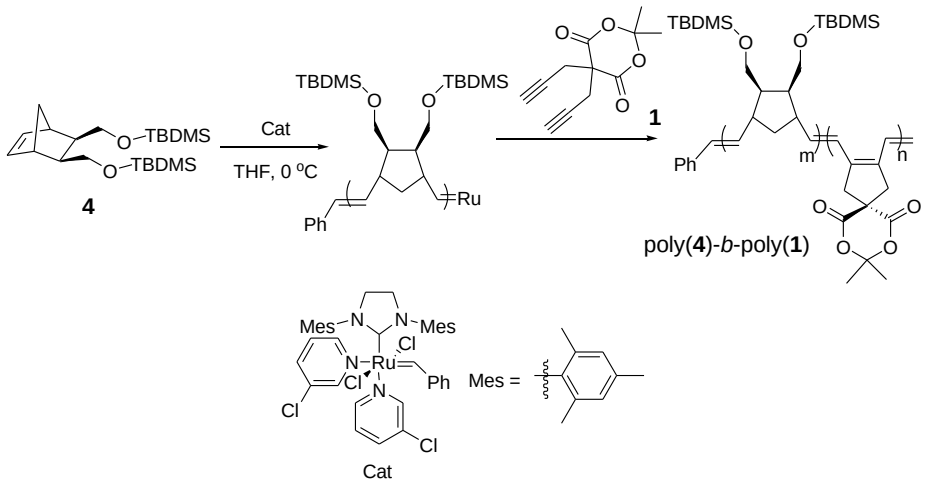

Scheme 2-2. Block copolymerization of *t*-butyldimethylsilylether substituted norbornene (**4**) and Meldrum's acid substituted 1,6-heptadiyne (**1**) using Grubb's 3rd catalyst.

First, we tried the analysis of optical property of the block copolymer, poly(**4**)$_{100}$-*b*-poly(**1**)$_{100}$, which was synthesized by ROMP and consecutive cyclopolymerization using UV–vis spectrum. At initial state, chloroform solution of poly(**4**)$_{100}$-*b*-poly(**1**)$_{100}$ showed blue-shifted and ill-defined absorption spectrum. After a few days, the same solution which was preserved under

light at ambient condition showed red-shifted spectrum and vibronic peak near 580nm (Figure 2-2). In addition, as time went by, bimodal spectrum became clear, and the intensity of both λmax near 520nm and vibronic peak increased. This solvent aging was accelerated by radiation of blue LED, and the UV–vis spectrum of solution aged by blue LED radiation showed the most well-defined absorption spectrum.

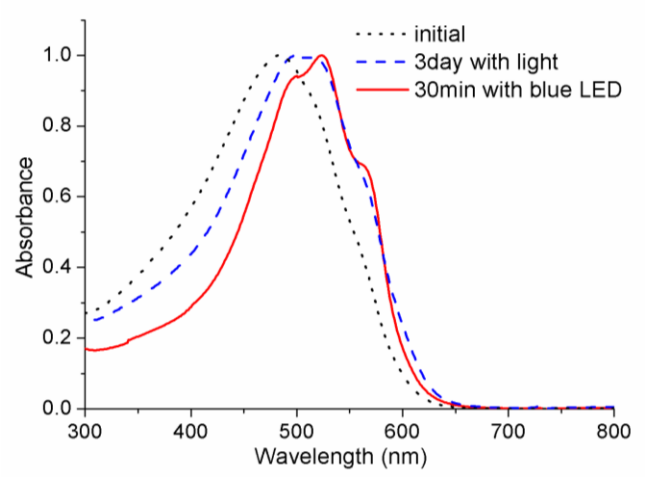

Figure 2-2. UV–vis absorption spectrum of poly(**4**)$_{100}$-*b*-poly(**1**)$_{100}$ by solvent aging (aging condition: 1g/l chloroform solution)

This change in UV–vis spectra represents the conformational change in the conjugated polymer backbone synthesized by cyclopolymerization. The increment in the intensity of vibronic peak, which is corresponding to the 0-0 transition of conjugated polymer, suggests that conformational structure of conjugated polymer is extended and planar.[22] So we expected the increment of the core size of spherical micelles as a result of the extended length of poly(**1**) chain by aging, and SEC, DLS, AFM, and TEM were used to analyze the nanostructure.

Interestingly, small core-shell structure formed larger particles as time went by, and the change of hydrodynamic diameter measured by DLS increased from 45.6nm to 100.4nm after 2 days of solvent aging using chlorobenzene (Figure 2-3). (THF and chloroform also showed the increment in the size, but there was variation in growth rate despite of the same aging time, concentration, and the intensity of light which was radiated.)

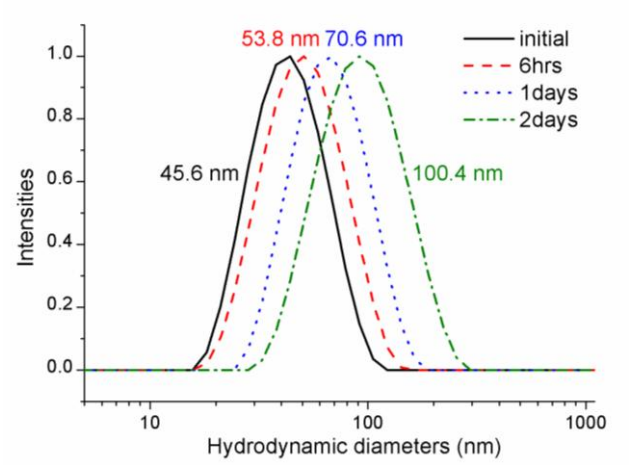

Figure 2-3. Change in hydrodynamic diameter in terms of solvent aging time. 1 g/l Chlorobenzene solution was held to the continuous light under ambient condition.

Doubled hydrodynamic diameter might not correspond to the size increment of core maintaining overall spherical core-shell structure, but the formation of the aggregate. To figure out actual nanostructure of the aggregate, atomic force microscopy (AFM) and transmission electron microscopy (TEM) were used. After a few days, spherical core-shell structures with the diameters of 20-30 nm formed nanocaterpillars which were linear, or Y-shaped (Figure 2-4). The length or nanocaterpillars increased in terms of aging time, and the number of branching point of Y-shaped one also increased.

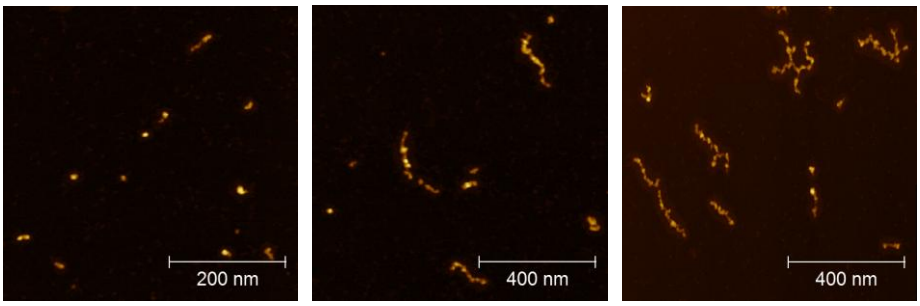

Initial 1 day 2 days

Figure 2-4. AFM images of nanostructures formed by in situ nanoparticle-zation of poly(**4**)$_{100}$-*b*-poly(**1**)$_{100}$ and solvent aging in terms of time. 0.1g/l chlorobenzene solutions were spincoated on mica at 3000 rpm for 1 min.

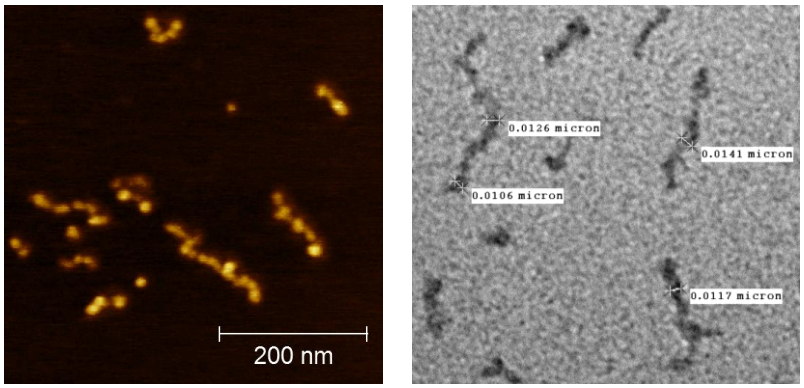

Figure 2-5. AFM and TEM images of poly(**4**)$_{100}$-*b*-poly(**1**)$_{100}$ aged for 3 days in chlorobenzene with light. 0.05 g/l chlorobenzene solution was spin-coated on mica (AFM) and 0.003 g/l solution was drop-casted on carbon grid.

By TEM image, it turned out that core consisting of conjugated polymer was connected to each other (Figure 2-5). Based on the interaction between core and hydrodynamic diameters measured by DLS, we concluded that these nanocaterpillars were existent even in solution state rather than derived from the aggregation on the surface of mica or grid during the sampling process. Previously, we reported similar nanocaterpillar structures prepared by in situ nanofabrication of poly-norbornene and polyacetylene block copolymer.[23] As the DP of PA block increased, block copolymer formed longer nanocaterpillar, while the one having the shortest PA block self-assembled affording to spherical core-shell structure.

Based on the result from UV–vis absorption spectrum, we concluded that poly(**1**) block which was extended by solvent aging generated driving forces of the nanocaterpillar formation. Extended poly(**1**) became more exposed to solvent affording to the interaction between micelles by solvophobic interaction and π-π staking of conjugated polymer core. Linear or Y-shaped nanocaterpillars rather than simply aggregated structure observed by AFM and TEM also supported that the previously reported mechanism of nanocaterpillar formation could be applied in this system.

Change in molecular weight measured by SEC also supported the formation of nanostructure which was larger than the initial core-shell structure. In the refractive index trace, the molecular weight of supramole-

cular adducts increased in terms of aging time, while the single chain of block copolymer maintained its retention time (Figure 2-6).

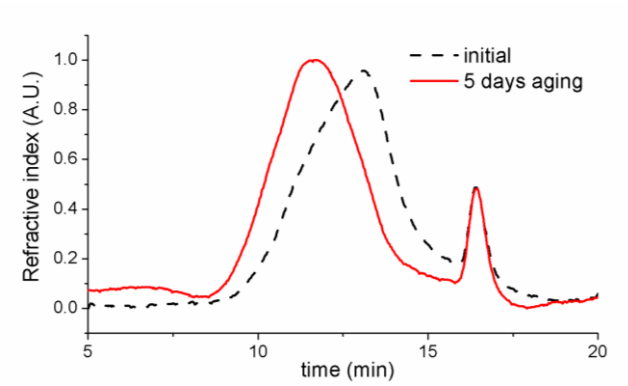

Figure 2-6. THF SEC traces of poly(**4**)$_{100}$-*b*-poly(**1**)$_{100}$ before and after aging in THF determined using an RI detector.

Conformational analysis using multi angle laser light scattering (MALLS) suggested the supramolecular adduct had worm-like structure after aging (Table 2-1). All of molecular weight, RMS radius, and hydrodynamic radius determined by light scattering and viscometry increased in terms of aging time. Moreover, the slope of RMS conformation plot also increased from 0.29 corresponding to the value for sphere to 0.47, and this increment might imply the conformation of supramolecular structure was close to random coil.[24] This analysis of the conformation of nanostructure was well-matched with the result from AFM and TEM, and both suggested that the interaction between spherical micelle was uni-directional affording to linear or Y-shaped nanocaterpillar.

Table 2-1. Conformational analysis of poly(**4**)$_{100}$-*b*-poly(**1**)$_{100}$ in terms of aging time determined using a THF MALLS detector.

time	Mn (kD)	R_{rms}	R_h	RMS conformation plot slope (α)
Initial	6,189	20.5	28.8	0.29
1 day	6,901	24.1	31.1	0.37
2 days	7,583	26.4	31.3	0.47
5 days	10,430	33.3	36.1	0.46

Nanocaterpillars detected by SEC implied that they maintain the nanostructure under SEC shear pressure, and the strong interaction at the interface of each micelle core was derived from the solvophobic interaction and π-π staking. To investigate the stability of the nanocaterpillar, further experiments using external stimuli such as sonication and heating were carried out (Figure 2-7). Firstly, nanocaterpillar with 139 nm of hydrodynamic diameter which was formed after 2 days of aging in chlorobenzene decomposed to smaller nanostructures after 1 hour of sonication (84.8 nm), and the decreased size was similar with the size of initial core-shell structure. It seemed that only the boundary was broken because the initial core-shell structure was not interfered by 1 hour of sonication. 1 hour after the sonication, separated micelle unit with exposed core formed much larger aggregate.

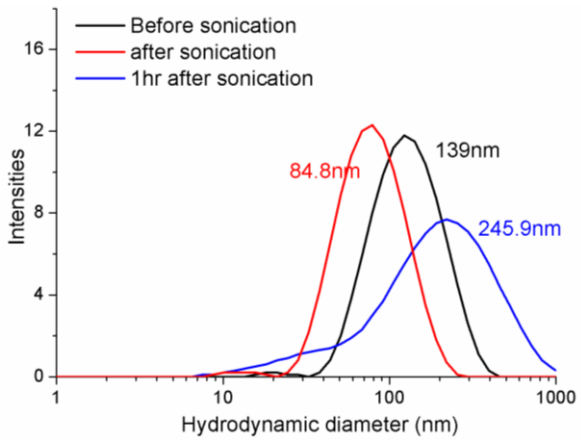

Figure 2-7. Change in the hydrodynamic diamters of nanostructure before and after sonication determined by DLS. Chlorobenzene solution of 2day aged poly(**4**)$_{100}$-*b*-poly(**1**)$_{100}$ underwent sonication for 1 hour at 40-50^{o}C

2day aged poly(**4**)$_{100}$-*b*-poly(**1**)$_{100}$ solution was heated at 60^{o}C and 100^{o}C for 2 hours and 1 1hour each, but small decrease in the size was observed. The hydrodynamic diameters decreased from 190 nm to 145-160 nm, but it did not decreased to its initial size (62.7 nm), while the sonication decomposed nanocaterpillar into the small spherical units. Moreover, even after 1 day of additional aging, the size was similar with that of the solution

before heating. This suggested the interaction in the boundary of each micelle core was too strong to be interfered by heating at 100°C.

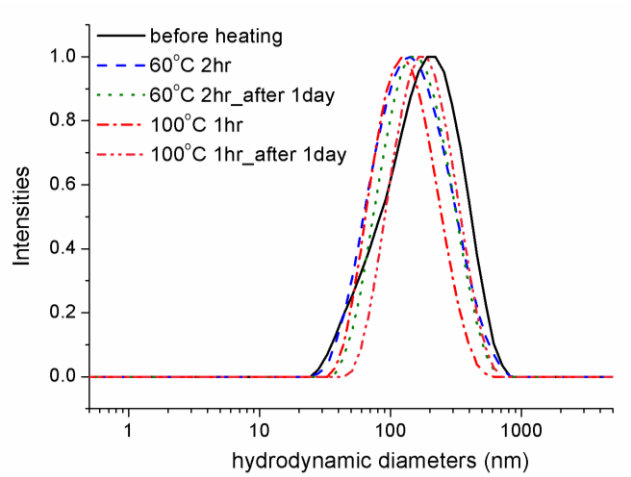

Figure 2-8. Change in the hydrodynamic diamters of nanostructure before and after heating determined by DLS.

Nanocaterpillar prepared by solvent aging showed good stability against external stilumi such as SEC shear pressure and heating except for the sonication which was the strongest. This stability was derived from the strong solvophobic effect based on the crystalinity of Meldrum's acid and solvophobicity of conjugated polymer backbone synthesized by cyclopolymerization. Moreover, increased π-π staking caused by solvent aging made the micelle units bound tightly.

2.4 Conclusion

In conclusion, we synthesized block copolymer with long Meldrum's acid substituted PA derivative by introducing more soluble comonomer. Block copolymer consisting of longer PA derivative block formed nanocaterpillar by the uni-directional interaction between spherical core-shell structures formed by in situ nanoparticilization. Solvophobic PA derivative which was extended by solvent aging exposed to solvent, and solvophobic interaction and additional π-π staking between the exposed core were the driving forces of nanoparticlization. This interaction at the boundary was strong to maintain the nanostructure against some external stimuli such as SEC shear pressure and heating to 100^{o}C. This stable nanocaterpillar could be useful as electronic materials consisting potentially conducting cores with insulating shells. Moreover, the process preparing nanocaterpillar is noteworthy because the length of nanostructure is easily controlled by the aging condition such as the intensity of light and aging time.

Reference

(1) Natta, G.; Mazzanti, G.; Corradini, P. Atti Accad. Naz. Lincei, Cl. Sci. Fis., Mat. Nat., Rend. **1958**, 25, 3.

(2) Chiang, C. K.; Druy, M. A.; Gau, S. C.; Heeger, A. J.; Louis, E. J.; MacDiarmid, A. G.; Park, Y. W.; Shirakawa, H. *J. Am. Chem. Soc.* **1978**, *100*, 1013.

(3) Choi, S.-K.; Gal, Y.-S.; Jin, S.-H.; Kim, H.-K. *Chem. Rev.* **2000**, *100*, 1645.

(4) (a) Fox, H. H.; Schrock, R. R. *Organometallics* **1992**, *11*, 2763 (b) Fox, H. H.; Wolf, M. O.; O'Dell, R.; Lin, B. L.; Schrock, R. R.; Wrighton, M. S. *J. Am. Chem. Soc.* **1994**, *116*, 2827.

(5) (a) Anders, U.; Nuyken, O.; Buchmeiser, M. R.; Wurst, K. *Angew. Chem., Int. Ed.* **2002**, *41*, 4044 (b) Kumar, P. S.; Wurst, K.; Buchmeiser, M. R. *J. Am. Chem. Soc.* **2009**, *131*, 387.

(6) Kang, E.-H.; Lee, I, S.; Choi, T.-L. *J. Am. Chem. Soc*. **2011**, *133*, 11904.

(7) Lee, I. S.; Kang, E.-H.; Choi, T.-L. *Chem. Sci.* **2012**, 3, 761.

(8) Meldrum, A. N. A. *J. Chem. Soc.* **1908**, *93*, 598.

(9) (a) Dumas, A. M.; Fillion, E. *Acc. Chem. Res.* **2010**, *43*, 440 (b) Gaber, A. E. M.; McNab, H. *Synthesis* **2001**, 2059.

(10) Leibfarth, F. A.; Kang, M.; Ham, M.; Kim, J.; Compos, L. M.; Gupta, N.; Moon, B.; Hawker, C. J. *Nat. Chem.* **2010**, *2*, 207.

(11) Miyamura, Y.; Park, C.; Kinbara, K.; Leibfarth, F. A.; Hawker, C. J.; Aida, T. *J. Am. Chem. Soc.* **2011**, *133*, 2840.

(12) (a) Nagai, D.; Sudo, A.; Endo, T. *Macromolecules* **2006**, *39*, 8898 (b) Spruell, J. M.; Wolffs, M.; Leibfarth, F. A.; Stahl, B. C.; Heo, J.; Connal, L. A.; Hu, J.; Hawker, C. J. *J. Am. Chem. Soc.* **2011**, *133*, 16698.

(13) **1** has been also homopolymerized by classical catalyst system, see Jin, S.-H.; Cho, H.-N.; Choi, S.-K. *J. Polym. Sci., Polym. Chem.* **1993**, *31*, 69.

(14) Blanazs, A.; Madsen, J.; Battaglia, G.; Ryan, A. J.; Armes, S. P. *J. Am Chem. Soc.* **2011**, *133*, 16581.

(15) (a) Kawa, M.; Fréchet, J. M. J. *Chem. Mater.* **1998**, *10*, 286. (b) Schubert, U. S.; Nuyken, O.; Hochwimmer, G. *Designed Monomers and Polymers* **2000**, *3*, 245. (c) Cave, R. A.; Seabrook, S. A.; Gidley, M. J.; Gilbert, R. G. *Biomacromolecules* **2009**, *10*, 2245..

(16) Li, Z.; Ma, J.; Lee, N. S.; Wooley, K. L. *J. Am. Chem. Soc.* **2011**, *133*, 1228.

(17) (a) Wang, H.; Wang, H. H.; Urban, V. S.; Littrell, K. C.; Thiyagarajan,

P.; Yu. L. *J. Am. Chem. Soc.* **2000**, *122*, 6855 (b) Park, S.-J.; Kang, S.-G.; Fryd, M.; Saven, J. G.; Park, S.-J. *J. Am. Chem. Soc.* **2010**, *132*, 9931.

(18) Patra, S. K.; Ahmed, R.; Whittell G. R.; Lunn, D. J.; Dunphy, E. L.; Winnik, M. A.; Manners, I. *J. Am. Chem. Soc.* **2011**, *133*, 8842.

(19) (a) Won, Y.-Y.; Davis, H. T.; Bates, F. S. *Science* **1999**, *283*, 960 (b) Piogé, S.; Nesterenko, A.; Brotons, G.; Pascual, S.; Fontaine, L.; Gaillard, C.; Nicol, E. *Macromolecules* **2011**, *44*, 594.

(20) O'Reilly, R. K.; Joralemon, M. J.; Wooley, K. L.; Hawker, C. J. *Chem. Mater.* **2005**, *17*, 5976.

(21) For further information of crosslink of micellar architectures, refer to; Rodríguez-Hernández, J.; Chécot, F.; Gnanou, Y.; Lecommandoux, S. *Prog. Polym. Sci.* **2005**, *30*, 691.

(22) Kang, E.-H.; Lee, I.-H.; Choi, T.-L. *ACS Macro Letters* **2012**, *1*, 1098

(23) Yoon, K.-Y.; Lee, I.-H.; Kim, K. O.; Jang, J.; Lee, E.; Choi, T.-L. *J. Am. Chem. Soc*. **2012**, *134*, 14291

(24) Conformation plot slope value: sphere (-0.3), random coil (0.5-0.6), rod (0.6-1.0), perfect rod (1.0)

국 문 초 록

Meldrum’s acid는 열분해에 의해 반응성이 좋은 작용기인 키틴기를 형성하는 선구물질로 여러 화학반응에 이용되어 왔다. 이 연구에서는, 그럽스 3세대 촉매를 사용한 싸이클로폴리머리제이션을 통해 Meldrum’s acid를 작용기로 갖는 전도성 고분자를 합성하였고, 합성된 고분자의 분자량 또한 잘 조절되었다.

Meldrum’s acid의 결정성이 크기 때문에, 싸이클로폴리머리-제이션을 통해 만든 폴리아세틸렌 유도체의 용해도가 증가하지 못했고, 이를 해결하기 위해 공중합을 이용하였다. 용해도가 좋은 단위체와의 공중합을 통해 Meldrum’s acid가 치환된 전도성 고분자를 포함하는 랜덤 공중합체와 블록 공중합체를 합성하는데 성공하였다. 블록 공중합체를 합성하는 과정에서 흥미로운 점을 발견하였는데, Meldrum’s acid를 포함한 전도성 고분자인 두 번째 블록이 자라면서 자발적으로 나노 입자를 형성하는 것이었다. 이는 용해도에 의해 잘 녹지 않는 두 번째 블록이 용매를 배척하는 것뿐 아니라, 자라나는 전도성 고분자의 π 결합 간의 상호작용으로 인해 두 번째 블록 간에 강한 인력이 작용하기 때문이다. 이러한 강력한 추진력으로 인해, 자기조립을 유도하기 위한 추가적인 처리 없이 블록 공중합체의 합성 과정 자체만으로도 매우 안정한 코어-셸 구조를 형성하게 되는 것이다.

게다가, 코어를 이루는 전도성 고분자는 Meldrum’s acid의 열분해를 통해 키틴기를 작용기로 갖게 되고, 연쇄적으로 일어나는 키틴기 간의 싸이클로어디션으로 코어에 크로스 링크가 만들어진, 훨씬 안정한 초분자체를 형성하게 된다. 이러한 일련의 과정은 적외선 분광법을 이용한 작용기의 확인으로 관찰하였다.

이러한 흥미로운 자기조립 현상을 바탕으로, 새로운 나노구조를 형성하기 위해 더 긴 길이의 잘 녹지 않는 두 번째 블록을 가진

블록 공중합체를 합성해 보았다. 두 번째 블록, 즉 폴리아세틸렌 유도체 부분이 충분히 길어지면 용매를 사용하여 에이징을 하였을 때 나노구조가 구형의 코어-셸 구조에서 나노캐터필러 형태로 변화하는 것을 확인하였다. 이러한 나노캐터필러의 형성 과정은 자외선/가시광선 흡수 스펙트럼과 사이즈 배제 크로마토그래피, 동적 광산란법, 그리고 원자현미경을 통해 관찰하였다. 또한, 코어 형태를 확실히 하기 위해 투과전자현미경도 사용하였다.

주요어: 싸이클로폴리머리제이션, Meldrum's acid, 전도성 고분자의 자발적인나노 입자화, 나노캐터필러

학 번: 2011-20289